13th AIAA/ISSMO Multidisciplinary Analysis Optimization Conference
13 - 15 September 2010, Fort Worth, Texas

AIAA 2010-9075

Enhanced Conceptual Wing Weight Estimation Through Structural Optimization and Simulation

Jason Petermeier[1], George Radtke[2], Matt Stohr[3], Aaron Woodland[4]
Dell Perot Systems, Plano, TX

Timothy T Takahashi[5], Shane Donovan[6]
Northrop Grumman Corporation, El Segundo, CA

Michael Shubert[7]
Dassault Systemes, Flower Mound, TX

This paper reviews the ability to create a design tool utilizing a combination of Microsoft Excel, Visual Basic for Applications, CATIA, and ABAQUS that is capable of providing an optimized wing structural weight and available fuel volume for a given wing planform with certain mission parameters. This calculated weight and volume is based on real structure and geometry as opposed to empirical and parametric equations that are based on historical data that may or may not be optimized or relevant. This design tool is also capable of providing internal wing structure geometry including 3D CAD models and finite element models that can be used to take the conceptual design into a preliminary design. Because of the fidelity of the structure that the design tool is able to generate, the conceptual design phase can be reduced from weeks and months to hours or days.

Nomenclature

A	=	Area
ABAQUS	=	Analysis software
Aero	=	Location of the aero load line
BL	=	Buttline
CATIA	=	3D CAD modeling software
CG	=	Center Of Gravity
Cp	=	Coefficient of pressure
E	=	Modulus of Elasticity
FS	=	Fuselage Station
g	=	Acceleration due to gravity
GTOW	=	Gross Takeoff Weight
GUI	=	Graphical User Interface
I	=	Moment of Inertia
Inertial	=	Location of the inertial load line
k	=	Fuel Volume Knockdown Factor

[1] Delivery Manager, Aerospace Engineering Department, Dell Engineering Services, Plano, TX, Senior Member AIAA
[2] Enginnering Advisor, Aerospace Engineering Department, Dell Engineering Services, Plano, TX, Member AIAA
[3] Lead Project Engineer, Aerospace Engineering Department, Dell Engineering Services, Plano, TX, Member AIAA
[4] Project Engineer, Aerospace Engineering Department, Dell Engineering Services, Plano, TX, Member AIAA
[5] Engineer 5, Configuration and Integration Department, Multi-Disciplinary Analysis and Optimization (MDAO) Project Team member, Northrop Grumman Aerospace Systems, El Segundo, Ca. presently Santa Clara University, Santa Clara, Ca. Associate Fellow AIAA
[6] Enginner 1, Aerodynamics Design and Analysis Department, Multi-Disciplinary Analysis and Optimization (MDAO) Project Team member Northrop Grumman Aerospace Systems, El Segundo, Member AIAA
[7] Prinicpal Engineer, Dassault Systemes, SIMULIA Southern Region, Flower Mound, TX

L = Length
LEFS = Leading Edge Fuselage Station
MDO = Multi-Discipline Design Optimization
Mx = Moment about the x-axis
My = Moment about the y-axis
Nx = Load factor in the x direction
Ny = Load factor in the y direction
Nz = Load factor in the z direction
OML = Outer Mold Line
P = Pressure
q = Shear Flow
REF = Location of the reference line of action
V = Volume
VBA = Visual Basic for Applications
W = Weight
WDT = Wing Design Tool
WL = Waterline
WS = Wing Station
SUI = Spreadsheet User Interface
ρ = Density
ω = Magnitude of aero load
φ = Angular roll rate

COORDINATE SYSTEM AND SIGN CONVENTION

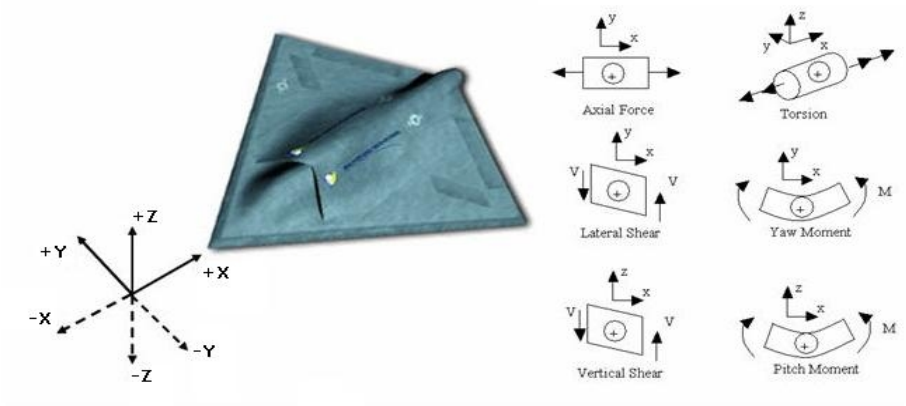

$+\alpha$ = nose up
$+\beta$ = port wing down

n_x = + aft load factor = $-a_x$ (longitudinal acceleration)
n_y = + starboard load factor = $-a_y$ (lateral acceleration)
n_z = + up load factor = $-a_z$ (vertical acceleration)

A_{xx} = radial acceleration about x-axis, + starboard wing up
A_{yy} = radial acceleration about y-axis, + nose up
A_{zz} = radial acceleration about z-axis, + nose port

I. Introduction

THE conceptual design of aircraft requires the accurate prediction of as-built characteristics given a set of design criteria. Typical weight estimations use an empirical regression analysis of historical aircraft to estimate the weight of internal structures. This method has a very short computational time and is well suited for design optimization; however, there are also significant drawbacks. First, is the assumption that the historical aircraft used to create the regression were all optimally designed. Second, the weight prediction is made without definition of an internal structure. This requires the design team to fit a structure into the weight requirement (or not). Lastly, regressions generally do not account for variations in internal layout. On the other hand, it is too time intensive for a team (or teams) of designers to draft structure across the entire design space. To address these concerns, a design tool was created to automate the initial structural sizing of an aircraft wing and provide weight prediction based on the verifiable structure.

An automated structural design method was developed by the authors to address these issues. For any given outer mould line geometry, a rule based formulation is used to develop an internal structural topology, and structural element sizing engineered to meet specific design load limits. This method (we call WDT – short for Wing Design Tool) may be coded in a straightforward high level language. In this case, VBA contained within Microsoft Excel. Microsoft Excel was chosen as a programming platform for integration due to its flexibility and universality; it also integrates smoothly into a multi-disciplinary trade study environment such as that offered by Phoenix Integration's ModelCenter.

To fully bound the design space in a single method requires that the WDT consider the input and integration of many disciplines. The initial goals were to address inputs from aero performance, configuration integration / layout, manufacturing, structures, loads, and cost estimating groups. For use in a systems concept design (MDO) process or in a preliminary structural design environment, computational time was an important consideration. Therefore, to provide insight, the automated structural design method was formulated around an optimization routine that would search for the lowest weight, structurally feasible wing. For verification of the resulting preliminary structural designs, tie-in's to directly export geometry, materials and loads to both CATIA and ABAQUS were created. The CATIA module is capable of producing surface and solid models of the wing structure. A dedicated ABAQUS plug-in automatically creates a surface model of the optimized wing for an FEA analysis.

Once the structural design method has been validated over a broad series of test problems, it may then serve in two capacities: 1) as a preliminary structural design tool to support the development of a specific configuration and 2) as a defined medium-to-high fidelity process to develop basis data to build "meta-models" of structural weight that can supersede the purely empirical weight equations used during concept design. More specifically, the team seeks to enable trades to determine the "best" mission performance for a given wing transverse design load. In this circumstance, an elliptical transverse lift distribution is most desirable from an aerodynamic drag perspective (a mono-disciplinary optimum solution), whereas an aerodynamically sub-optimal span loading might be offset by savings in wing structural weight to produce a smaller, lighter vehicle. This paper describes the method alone, applications of this method in a general systems design context will be discussed in future manuscripts.

II. Methodology

The WDT was created in Microsoft Excel 2007. A spreadsheet user interface (SUI) was created to accept inputs and output results. An optimization technique was developed to search for the least weight structurally feasible topology for the specified requirements. Optimization was executed through a set of macros programmed in VBA for Excel. To verify resultant structures, tie-ins were created with CATIA and ABAQUS. Automated surface and solid CATIA models were scripted using VBA macros. FEA verification is aided by an automated ABAQUS model scripted in Python.

A. User Interface

Inputs to the WDT are organized on four separate worksheets; Geometry Definition, Constraints, Loads, and Airfoils. Figure 1 shows the worksheets and data-flow of the design tool. Geometry definition includes all the top level inputs required in the problem set-up. Basic planform, control surface, spar, payload, landing gear, fixed rib locations, and fuel tank parameters are entered here. While the planform geometry and parameters are being entered, a 2D representation of the wing is displayed to aid in the placement of components. Also, an embedded button exists to create a CATIA surface model that allows the user to review their wing design before the optimization process takes place.

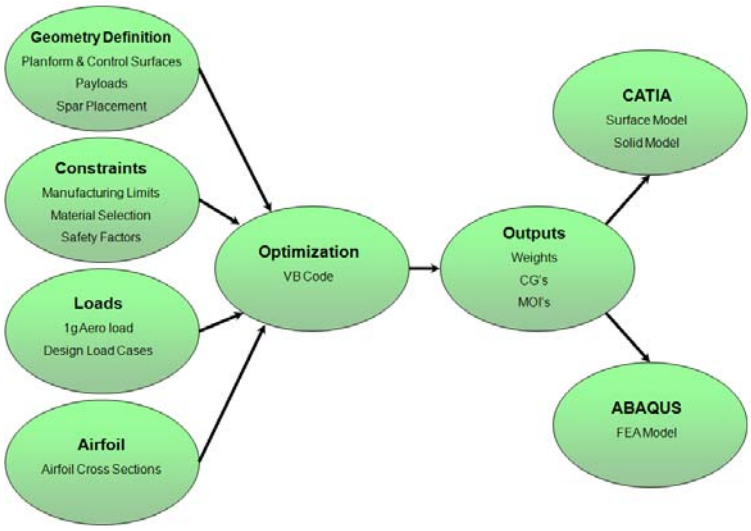

Figure 1. Design Tool Interface

Wing planform is defined by eight unique control points (Fig. 2). Together the control points allow any combination of chord, sweep, taper, dihedral, and twist to be created. Each control point is also assigned an airfoil. Airfoil definitions are input normalized to a chord length of one. Using the control point inputs and airfoil cross-sections the wing OML is defined.

Up to seven trailing edge control surfaces can be toggled on and off (Fig. 3). Spanwise, each control surface is defined between two adjacent planform control points. Chordwise, each is defined by a percent chord at the inboard and outboard limits. Control surface geometry is used to define keep out zones for other wing structures and provide weight tracking for trailing edge components.

A minimum of two main spars, a forward and an aft spar, must be defined for an analysis (Fig. 3). Up to four intermediate spars may be toggled on and off. Each spar is defined by three control points; root, variable and tip. The root and tip control points are locked spanwise in their respective positions. The variable control point can be placed at any specified BL position to allow for breaks in the structure. An auxiliary spar is optional and can be toggled on and off. The auxiliary spar tip placement is defined by the intersection of the aft spar with a user input BL position. Root placement is at side of body such that the auxiliary spar attaches to landing gear positioned behind the aft spar.

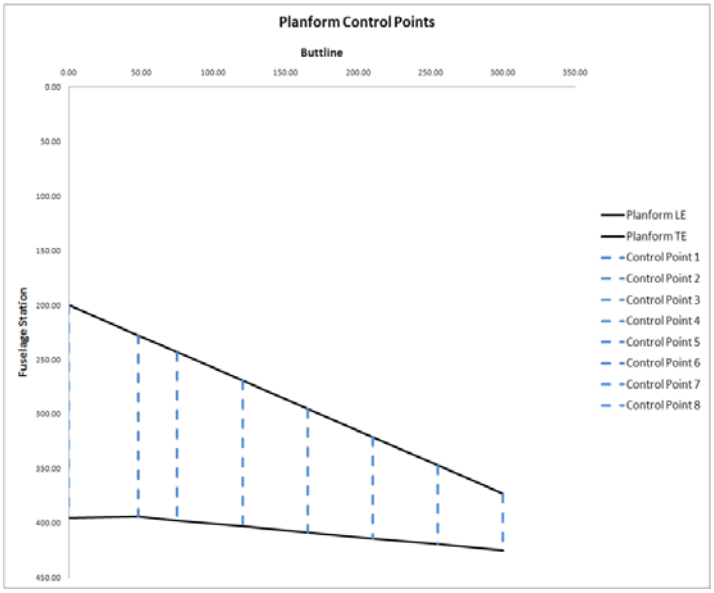

Figure 2. Wing Planform Control Points

A payload may be defined as an internal or external store. Each is characterized by its CG position, length, width, height, and weight. Depending on the type of payload a structural option may be toggled on and off. This option determines if the wing skins react any load or if other structures need to account for the loading. A total of four payloads may be input to the design tool.

Landing gear geometry can be toggled on and off for aircraft that require wing stored gear (Fig. 4). The keep out zone is defined by a four sided polygon attached to the aft spar. Each dimension may be modified independently. Gear may be placed either in front or behind the aft spar and at any spanwise location on the wing.

Based on the wing planform and system requirements, a series of pre-defined fixed ribs are located along the span (Fig. 4). A minimum of two fixed ribs, the wing root and tip, are required to begin optimization. Additional ribs are placed at key structural points including payloads, landing gear, spar discontinuities, fuel tank termination points, and aircraft side of body.

For a wet wing, multiple fuel tanks may be created along the span. Tank volumes are defined by an inboard rib, outboard rib, forward spar, and aft spar. The inboard and outboard ribs are selected from the list of fixed ribs. Each fixed rib can be toggled on or off as a fuel termination rib. When two fixed ribs are called out as fuel terminating ribs, a tank is created between them.

Airfoil cross sections are input and stored on the airfoils worksheet. Together the geometry definition and airfoil worksheets encompass all the data required to establish the final geometry needed for the optimization process to take place.

Additional constraints are available to reduce the scope of the design space. These parameters are accessible through the constraints worksheet. Here the user can establish manufacturing limits on the wing. Limits include minimum and maximum component thicknesses, rib spacing, and stiffener spacing. These limits reduce the design space searched by the optimization code to improve the computational run time. Material assignments are also called out via the constraints worksheet on a component level (spars, ribs, upper skins, lower skins). This worksheet also contains a material library so the user can quickly select different material assignments for the various wing components.

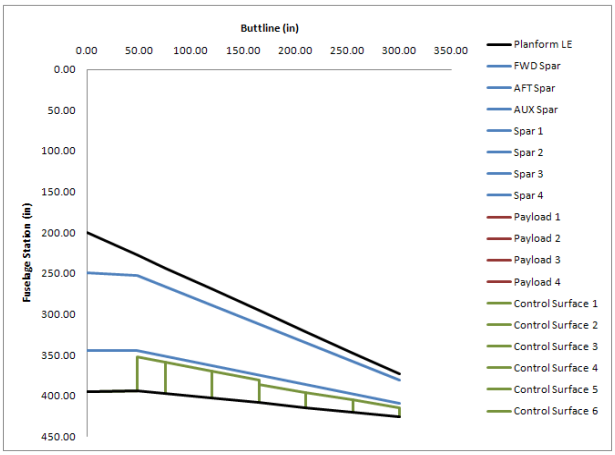

Figure 3. Control Surface and Spar Placement

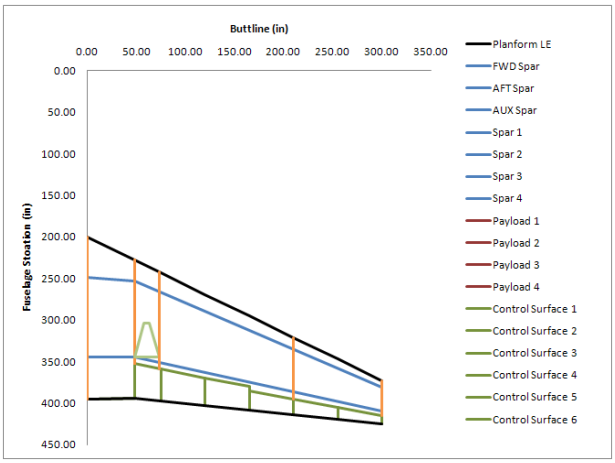

Figure 4. Landing Gear and Fixed Rib Placement

To track the load inputs and calculate design load cases, a dedicated loads worksheet was created. Required load inputs are a 1-g cruise aero line load and the design load cases.

B. Loads Calculations

The design tool accounts for four inertial (mass) loads and one aerodynamic load. The four inertial loads include fuel weight, wing structure, payloads, and landing gear reactions. Every load is calculated as a line load at one inch increments along the span. Line of action for each load may be different depending on the configuration. Up to seven design load cases can be specified. Each can be independently configured to represent different parts of the flight envelope. The design loads are calculated in a four step process. First the aero and inertial loads are determined for a 1-g cruise flight condition. Next, the 1-g loads are scaled by each load case and the fuel pressure loads are calculated. In the third step total load, shear, Mx, and My are calculated for each load case. Last, the design loads are compiled as the maximum value for total load, shear, Mx, and My at each BL position.

An initial estimate for the wing structure weight is made through empirical formulae. This weight is assumed to be linearly distributed (eq. 1) from the wing root to tip (Fig. 5).

$$WingWeight(BL) = \frac{(2)\times(guess)\times(BL)}{(BL_{\max}{}^{2})} - \frac{(2)\times(guess)}{BL_{\max}} \quad (1)$$

1. Fuel Weights

Fuel weight is calculated for each tank defined by the user inputs. Using the airfoil control points a cross-sectional area is calculated for each wing station. The cross-sectional area of the fuel tank at the inboard and outboard terminating BL positions is calculated by linear interpolation between the wing station areas (eq. 2).

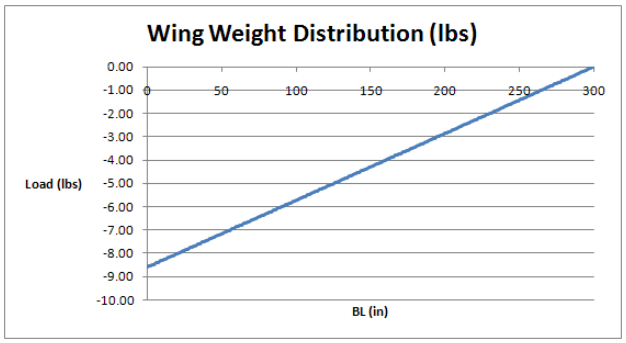

Figure 5. Linear Weight Distribution

$$A(BL) = \frac{\left(A_{WS\_2} - A_{WS\_1}\right)}{\left(BL_{WS\_2} - BL_{WS\_1}\right)} \times \left(BL - BL_{WS\_1}\right) + A_{WS\_1} \tag{2}$$

The cross-sectional area of the tank is then calculated as the average of the inboard and outboard cross-sectional areas (eq. 3).

$$A_{tank} = \frac{A\left(BL_{inboard}\right) + A\left(BL_{outboard}\right)}{2} \tag{3}$$

The span of the tank is measured along a reference line located midway between the forward and aft spar. A raw OML tank volume is calculated as a function of tank area and span. To account for internal structures a knockdown factor (k) is applied to the tank volume calculation (eq. 4).

$$V_{tank} = \left(A_{tank}\right) \times \left(L_{tank}\right) \times \left(k\right) \tag{4}$$

Tank volume is then multiplied by the fuel density to determine fuel weight in the tank (eq. 5). The fuel weight is assumed to be evenly distributed from the inboard to outboard tank termination BL (Fig. 6).

$$W_{fuel} = \left(V_{tank}\right) \times \left(\rho_{fuel}\right) \tag{5}$$

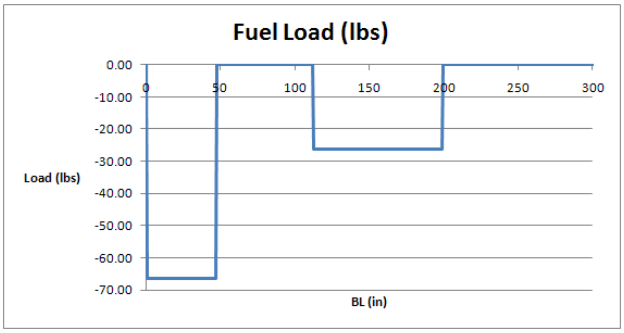

Figure 6. Distributed Fuel Load

2. Payloads

Each payload is specified as either internal or external. An internal payload weight is assumed to be evenly distributed between its inboard and outboard payload BL positions. Loads for external payloads are applied at the payload CG BL position (Fig. 7).

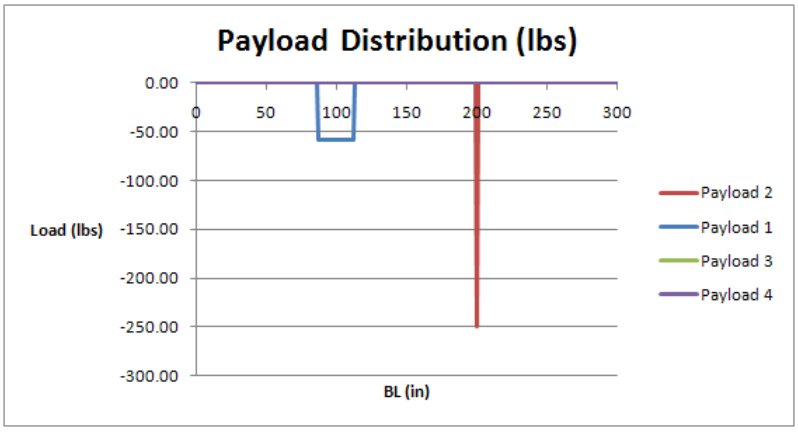

Figure 7. Internal / External Payload Distribution

3. Landing Gear Loads

Landing gear loads are calculated as point loads at the inboard and outboard landing gear rib BL positions. Load applied to each main gear (left and right) is assumed to be half of GTOW. One half the gear load is applied to each landing gear rib, calculation shown in Eq. (6).

$$LandingGear_{1g} = \frac{GTOW}{4} \tag{6}$$

4. Aero Loads

The 1-g aero load can be input one of two ways. If the load is known through a CFD code it can be entered manually by the user. In the case where the load is not yet known it is assumed to be elliptical (Eq. 7). The magnitude (ω) of the aero load is scaled until shear at the wing root is equal to the GTOW of the aircraft simulating a 1-g cruise condition.

$$Aero_{1g}(BL) = \sqrt{\left(1 - \left(\frac{BL}{BL_{tip}}\right)^2\right) \times \left(\omega^2\right)} \tag{7}$$

5. Load Case Scaling

Up to seven load cases can be analyzed for each wing optimization (Fig. 8). Payload and landing loads may be cycled on or off for each load case. The percent fuel can be varied from 0% to 100%. Load factors in the x, y, and z directions along with a roll rate are also required inputs. Only the Nz load factor and %fuel are required to scale the aero and inertial loads. The Nx, Ny, Nz, and roll rate are used to calculate fuel head pressures.

Load Case 1		
Landing	0.00	1=yes
%Fuel	60%	
Payload	0.00	1=yes
Nx	1.25	g
Ny	0.25	g
Nz	7.50	g
Roll Rate	0.00	rad/sec

Figure 8. Sample Load Case Inputs

$$Aero(BL) = Aero_{1g}(BL) \times (Nz) \quad (8)$$

$$WingWeight = WingWeight_{1g} \times (Nz) \quad (9)$$

$$PayloadWeight = PayloadWeight_{1g} \times (Nz) \quad (10)$$

$$FuelWeight = (FuelWeight_{1g}) \times (\%fuel) \times (Nz) \quad (11)$$

$$LandingGear = LandingGear_{1g} \times (Nz) \quad (12)$$

6. Fuel Pressure Calculations

Ultimate fuel pressure is calculated at each one inch BL increment. Hydrostatic pressure induced by the roll rate and load factors is accounted for. Tank geometry is defined in Fig. 9.

The lengths in the x, y, and z directions represent maximum possible internal tank length in their respective directions. Endpoint locations for these measurements may change depending on planform geometry and is accounted for in the WDT. Combining the geometrical lengths with the load factors in their respective directions the hydrostatic pressure due to load factors can be found using Eq. 13.

Lengths Lo and Li are measured from the center of rotation (assumed at centerline, BL=0). The difference in lengths is combined with angular roll rate to determine maximum hydrostatic pressure in Eq. 14.

Addition of the pressure due to load factors and roll rate yields the total hydrostatic pressure induced at each BL position along the wing.

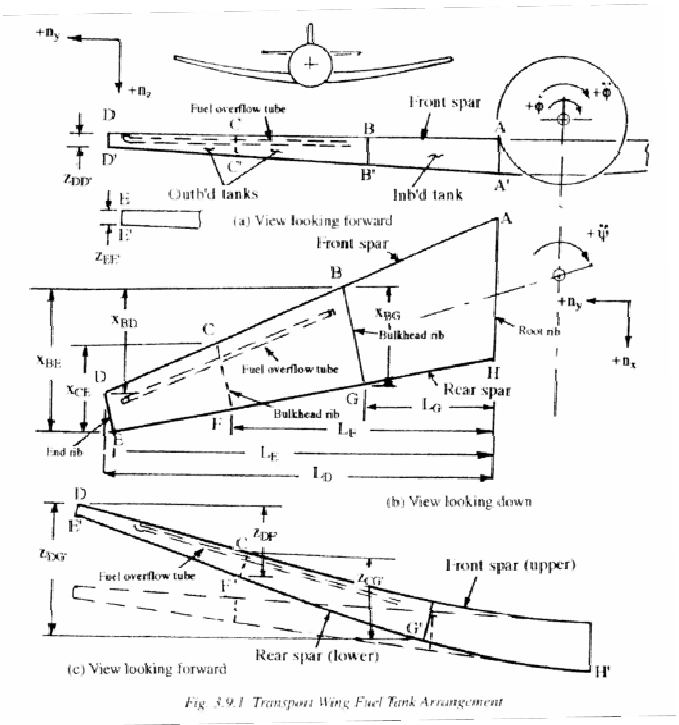

Figure 9. Fuel Tank Pressure Calculation Diagram [1]

$$P = 1.5\left[\left(n_x \times L_x + n_y \times L_y + n_z \times L_z\right) \times \rho\right] \tag{13}$$

$$P = 1.5\left[\left(\frac{\phi^2}{2g}\right) \times \left(L_o^2 - L_i^2\right) \times \rho\right] \tag{14}$$

7. Shear and Moment Calculations

To develop shear and moment profiles a line of action is defined for the aero and inertial line loads. The aero line of action defaults to quarter chord unless otherwise specified by the user. Fuel and initial wing weight inertial loads have a common line of action defined halfway between the forward and aft spars. Effects of payload weights are accounted for individually by their CG location. All calculations are made about a reference line co-linear with the inertial load line of action (Fig. 10).

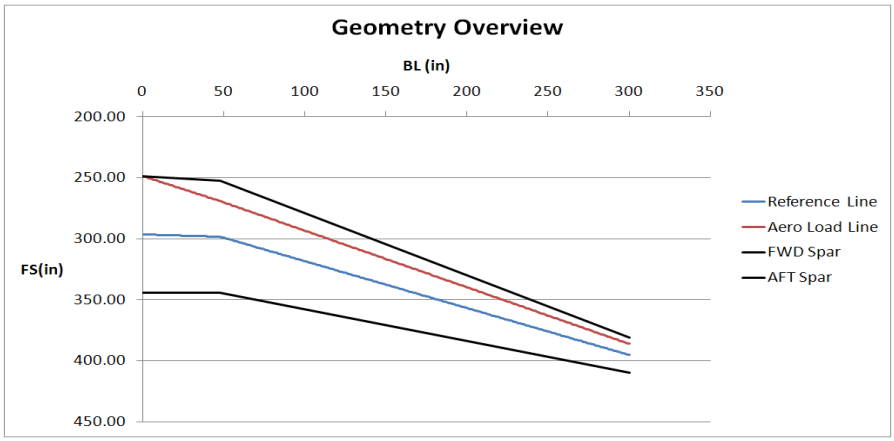

Figure 10. Reference / Aero Lines of Action

The total load is calculated as the summation of all Aero and inertial loads by BL position (eq. 15).

$$TotalLoad(BL) = Aero(BL) + WingWeight(BL) + PayloadWeight(BL) + FuelWeight(BL) + LandingGear(BL) \quad (15)$$

Shear at each BL position (eq. 16)

$$Shear(BL) = \sum_{i=BL}^{BL\_max} TotalLoad(i) \quad (16)$$

Bending moment, Mx calc. (eq. 17)

$$Moment\_x(BL) = \sum_{i=BL}^{BL\_max} (TotalLoad(i)) \times (i - BL) \quad (17)$$

Torque, My calculation (eq. 18)

$$Moment\_y(BL) = \sum_{i=BL}^{BL\_max} (Aero(i) - REF(BL)) \times (Aero(i)) + (Inertial(i) - REF(BL)) \times (WingWeight(i) + FuelWeight(i)) \quad (18)$$

C. Optimization Procedure

The optimization procedure is based on a discretization of the wing into sections. Each section is divided into individual wing boxes between consecutive ribs. A preliminary analysis is made to size the structure in each wing box (see Section II: D– Structural Calculations). The result of these calculations determines if there are structurally feasible solutions, and if so which solution is the lowest weight option. Additional ribs are then added to the section and the structure re-sized. The weights of various rib configurations are tested to find the least weight option for the wing section. Total wing weight is determined by the addition of each section's least weight solution. A step by step breakdown of the procedure is described below.

1. Discretization

Initial discretization of the wing is performed with the fixed rib geometry defined in the problem set up. Each pair of fixed ribs defines a section to be analyzed. Section one is defined by the root rib and the next rib outboard. Each successive section is located outboard until the tip rib is reached (Fig. 11).

2. The Wing Box

A wing box is defined by the forward spar, aft spar, upper skin, lower skin, inboard rib and outboard rib. These components make up the torque box which reacts the applied loads to the wing root and fuselage.

3. Component Sizing

Each wing box structure is sized independently to support the loads experienced at the local BL position on the wing. Upper and lower skin structures are first sized with and without stiffeners. Rib geometry and spar geometry are then sized to determine cap thickness, web thickness, and stiffener geometries required. The least weight results for the wing box are stored for future comparison.

4. Iteration / Adding Ribs

The preliminary layout from the problem statement is broken up into sections defined by the fixed ribs. The number of ribs in each section is optimized independently from the other sections. Sections are analyzed from root to tip. The first analysis treats the section as a single wing box. Components are sized and the total weight (wt_1) is recorded. This process is shown in Fig. 12.

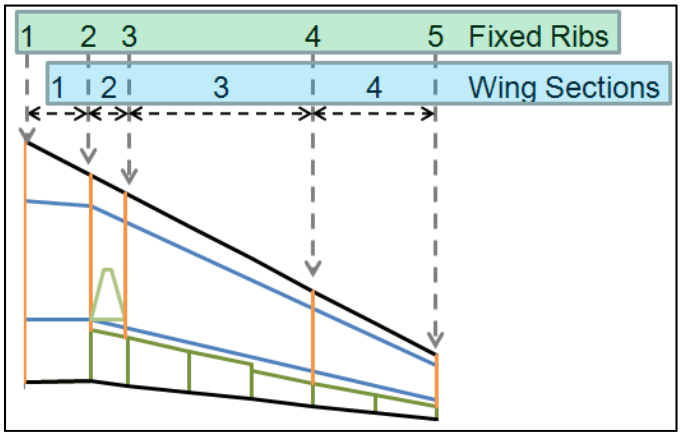

Figure 11. Fixed Rib Bay Definition

After analyzing a one wing box configuration, the same section is analyzed with the addition of a second wing box. A third rib is placed halfway between the inboard and outboard BL positions creating wing box 2a and wing box 2b. Structural calculations are made to size the components and record the weight of each wing box. The total weight of the section, wt_2 in Fig. 12, is calculated by addition of the wing box weights (wt_2a + wt_2b). If wt_2 is greater than wt_1, wt_1 is determined to be the optimal solution and the optimization is concluded. If wt_2 is less than wt_1 the optimization continues by placing a fourth rib into the wing section. The addition of a fourth rib divides the section into 3 rib bays. Again, the structural calculations are made and wt_3 is computed by addition of wt_3a, wt_3b, and wt_3c. Wt_3 is then compared with wt_2 from the previous step. If wt_3 is greater than wt_2, wt_2 is determined to be the optimal solution and the optimization is concluded. If wt_3 is less than wt_2 the optimization continues with the addition of another rib

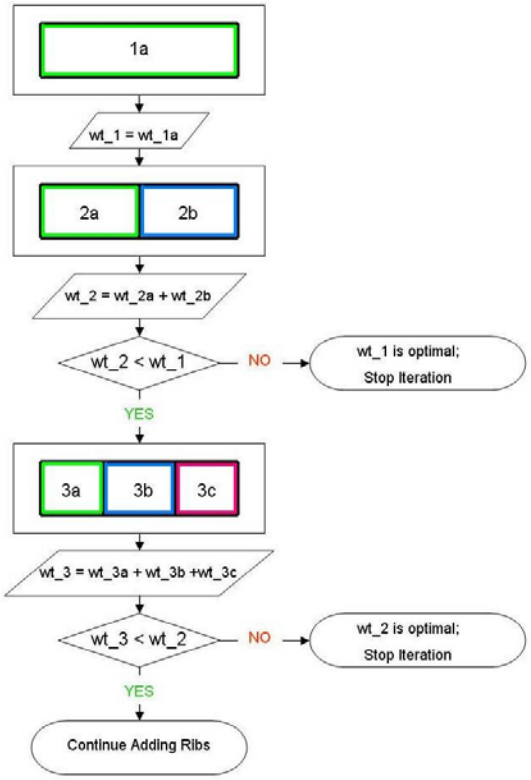

Figure 12. Rib Bay Iteration Process

to the section. The iterations continue this pattern of adding ribs, calculating weights and comparing results to arrive at the final least weight solution.

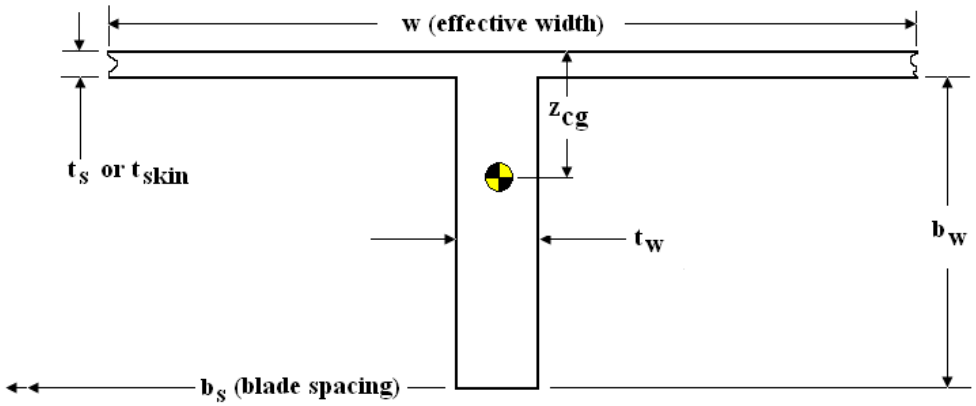

Figure 13. Integrally Machined Stiffened Panel Geometry

D. Structural Calculations

The internal wing structure components are idealized as integrally machined stiffened panels. This configuration was chosen as the basis for optimization due to the competitive cost of the manufacturing method and for the structural efficiency afforded by the stiffened panel geometry. In all cases, the geometry consists of a web or skin, stiffened as shown in Fig. 13.

1. Skins Methods and Equations

The skins are sized based on the wing bending load and internal fuel pressure. In the case of the wing bending load, both compression and tension loads are utilized.

Initially, the skins are assumed to be un-stiffened flat panels with pinned edges whose boundaries are defined by the spars and ribs for the rib-bay being evaluated. For the compression loaded skin, buckling is considered the critical condition. For the tension loaded skin, the skin is evaluated with a combination of tension due to bending and tension generated by the hydrostatic fuel pressure. A panel weight is calculated for this geometry and is stored as the initial skin panel weight.

Stiffeners are then added to the panel geometry where skin thickness, stiffener width, stiffener spacing, and stiffener height are all variables to be evaluated in the optimization matrix. Each input is varied from the minimum to maximum values defined in the constraints spreadsheet. For any given combination of stiffener geometry, a compression buckling check with and without fuel pressure and a tension check with and without fuel pressure is performed for both the stiffeners individually, and then for the skin panel bounded by the stiffener spacing and rib spacing of the panel of interest.

For a stiffener section being evaluated for buckling:

$$p_{critical} = \frac{3.14^2 (E)(I)}{(stiffener\_length)^2} \qquad (19)$$

Correspondingly, the supported skin is evaluated for buckling:

$$F_{ccr} = (3.62)(E)\left(\frac{t\_skin}{stiffener\_spacing}\right)^2 \quad (20)$$

A tension check is performed using tensile stress due to wing bending combined with tensile stress due to fuel hydrostatic pressure load:

$$w_{fuel} = \frac{(fuel\_pressure)(chord)}{num\_stiffener} \quad (21)$$

$$M_{\max} = \frac{(w\_fuel)(stiffener\_length)^2}{8} \quad (22)$$

For any combination of skin stiffened geometry which returns a positive margin for all the criteria outlined above, the weight is evaluated and compared to the un-stiffened panel baseline calculation. The lowest weight configuration with positive margin is recorded and returned to the spreadsheet.

2. Spar Methods and Equations

The spars are sized based on wing bending load, wing torsion load, and internal hydrostatic fuel pressure. In the case of the wing bending load, both compression and tension loads are utilized. In the case of the wing torsion load, the shear stress is conservatively assumed to be carried by the forward and aft spar only. Intermediate spar webs are not sized based on wing torsion.

The forward and aft spar webs are evaluated for torsion and bending where:

$$q_t = \frac{(\pm 1)(My)}{2A} \quad (23)$$

$$q_b = \frac{Vz}{spar\_height} \quad (24)$$

The spar webs are initially sized based on a shear resistant web sizing approach. For any given combination of web thickness, stiffener width, and stiffener spacing that fits within the constraints of the shear resistant web geometry criteria, margins are calculated. Stiffener height is set equal to the spar cap width. Once a positive margin is calculated, the spar web is checked for fuel pressure if it is located in fuel tank.

An identical calculation for fuel pressure loading for the skins is performed for the shear resistant spar web geometry. In the event that the fuel pressure load produces stresses exceeding the stiffener capabilities, the stiffeners are thickened until a positive margin is found. The least weight spar geometry and weight is then recorded and returned to the spreadsheet.

The spar caps are sized based on a load sharing coefficient determined by the combined spar cap widths and wing chord at the rib-bay being evaluated. Cap thickness is the only variable in this calculation. The spar cap width

is a user defined parameter entered as a geometry constraint. A cap thickness is then calculated which satisfies the maximum allowable tensile and compression stress produced by the wing bending load.

3. Rib Methods and Equations

The ribs are sized based on compression due to wing bending load and aerodynamic pressure loading. Additionally, the fuel termination ribs are sized based on internal hydrostatic fuel pressure.

The rib caps are first sized based on a user input cap width. The aerodynamic pressure loading that is beamed to the ribs from the skins is used to size the rib cap thickness. For a given rib-bay and rib spacing, the distributed cap loading is taken as the reaction at the rib station produced by the adjacent skins. The cap thickness is then easily determined where the rib is represented by a simply supported beam (supports at the forward and aft spar attachments). For those ribs which represent an engine mount, landing gear mount, or payload stores, an additional distributed load is applied to the rib beam equal to the inertial load produced by the respective implement.

The rib webs are sized identically to the spar webs using a shear resistant web approach. For those ribs which occur at a fuel termination, an additional calculation is performed to account for the fuel hydrostatic pressure loading. In addition to these effects, a compression load is induced into the ribs due to the wing bending (curvature). A compression buckling calculation both with and without fuel hydrostatic pressure loading is also performed. The same calculation procedure for calculating compression on the skins is performed for the ribs in this step. Following the iterations the lowest weight rib geometry is then retruned to the spreadsheet.

E. Output Summaries

After the optimization has been completed the WDT automatically displays the outputs worksheet. A primary summary table documents the empty weight, primary and secondary structures breakdown, available fuel, and tip deflection at 1-g cruise. Detailed mass properties are displayed for four flight conditions; no fuel with no payload, no fuel with max payload, max fuel with no payload, and max fuel with max payload. Under each flight condition the weight, CG and radii of gyration are displayed. For cost estimation, a material, parts count, and weight of material used for each type of structure are supplied. Material and weight of material used is displayed for each component group. A sample summary table is provided in Fig. 14.

Summary		
Overall Empty Weight	1008.46	lbs
Primary Structure	849.47	lbs
Secondary Structure	159.00	lbs
Fuel		
Fuel Volume	1189.99	gal
Fuel Capacity	7972.94	lbs
Payloads		
Payload 1	0.00	lbs
Payload 2	0.00	lbs
Payload 3	0.00	lbs
Payload 4	0.00	lbs
Tip Deflection	1.51	in

Flight Condition 1		
Empty / No Payload		
Wing Weight	1008.46	lbs
Wing Center of Gravity		
FS	319.8	in
BL	102.3	in
WL	0.0	in
Wing Radii of Gyration		
K_xx	73.48	in
K_yy	42.74	in
K_zz	85.02	in

Figure 14. Sample Output Display

III. Application

A. Planform Trade Study

A trade study was completed to study the effects of various input parameters on the WDT. The baseline wing had a 50ft span, two spars, fifteen total ribs, three fuel tanks and 25,000 lbs GTOW (for further details see Section IV – Verification). Six WDT results, including the baseline, were compiled. Variations to the baseline trial included changes in GTOW, OML thickness, design load cases, materials selection, and span. A summary of each trade is listed in Table 1.

Table 1. Trade Study Paramter Variations

Trade #1, Baseline:
50 ft span, 2 spars, 5 fixed ribs, fuel to BL 210, MTOW of 25,000 lbs, Al 7475 and Al 2024, transport (3g) load cases, baseline OML thickness.
Trade #2, Increased MTOW:
50 ft span, 2 spars, 5 fixed ribs, fuel to BL 210, MTOW of 30,000 lbs, Al 7475 and Al 2024, transport (3g) load cases, baseline OML thickness.
Trade #3, Increase OML Thickness:
50 ft span, 2 spars, 5 fixed ribs, fuel to BL 210, MTOW of 25,000 lbs, Al 7475 and Al 2024, transport (3g) load cases, OML thickness increased 1%.
Trade #4, Aerobatic Design Load Cases:
50 ft span, 2 spars, 5 fixed ribs, fuel to BL 210, MTOW of 25,000 lbs, Al 7475 and Al 2024, aerobatic / carrier load cases, baseline OML thickness.
Trade #5, Change Materials Selection:
50 ft span, 2 spars, 5 fixed ribs, fuel to BL 210, MTOW of 25,000 lbs, IM7/977-2 quasi isotropic skins, Ti-6-6-2 anl ribs, transport (3g) load cases, baseline OML thickness.
Trade #6, Span Increased 10%:
55 ft span (reference area held constant), 2 spars, 5 fixed ribs, fuel to BL 210, MTOW of 25,000 lbs, Al 7475 and Al 2024, transport (3g) load cases, baseline OML thickness.

For each trade, the WDT was run and CATIA models were created. The initial baseline model had an empty weight of 1,008 lbs, fuel capacity of 7,972 lbs, 1-g tip deflection of 1.51 inches and fifteen total ribs. A summary table with the effects of each trade on these results is displayed in Table 2.

Table 2. Trade Study Results Summary

	#1 Baseline 25K MTOW	#2 +5K MTOW	#3 +1% OML	#4 Aerobatic Loads	#5 Materials Change	#6 +10% Span
Empty Weight (lbs)	1,008	1,056	1,026	1,346	868	1,057
Fuel Capacity (lbs)	7,972	7,693	8,562	7,905	7,971	7,801
1g Tip Deflection (in)	1.51	1.83	1.27	1.31	1.76	2.85
# Ribs	15	15	15	21	13	17
CG_x	290.4	290.5	290.2	291.2	289.3	290.6
CG_y	27.2	27.4	26.8	29.2	24.6	27.1
CG_z	0.0	0.0	0.0	0.0	0.0	0.0
K_xx	34.6	34.9	33.9	37.4	29.2	37.3
K_yy	17.1	17.5	16.7	18.9	14.3	17.8
K_zz	38.6	39.0	37.7	42.0	32.5	41.4

Center of gravity and radii of gyration for max fuel / max payload conditions
Value Increased
Value Decreased

B. Automated CATIA Model

Three separate CATIA models may be created using the design tool. Each model is push button generated using VB code in Excel. The first model generated is an un-optimized skeleton model (Fig. 15). This model is a surface representation of the wing skins, spars, control surfaces, landing gear, fixed ribs, and payloads. During the lay-out of a potential planform this model provides a quick reference to a full three dimensional representation. Payload placements can be checked for interference with the wing OML and fixed internal structures.

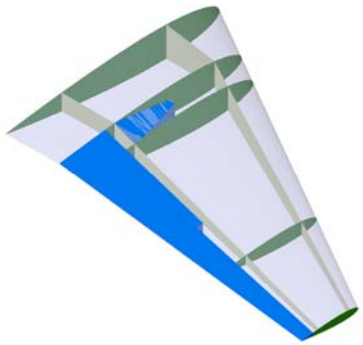

Figure 15. CATIA Un-Optimized Surface Model

The second CATIA model creates a skeleton of the optimized planform (Fig. 16). Skins, spars and ribs are modeled at mid-plane. This model allows the designer to review the optimized wing structure in three dimensions. Potential irregularities such as very dense or sparse rib placement can be spotted here for further investigation. The optimized surface model may also be used as the basis for a FEA surface/shell model.

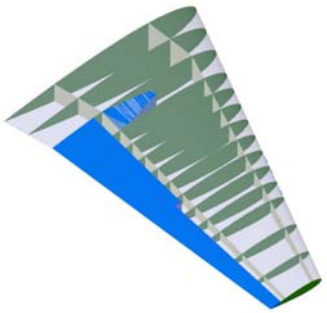

Figure 16. CATIA Optimized Surface Model

The third CATIA model creates a solid representation of the optimized wing structure (Fig. 17). Component web, cap and stiffener geometries taken from the design tool are passed into CATIA. Individual parts are created for each major component. An assembly file then loads the individual components and assembles them into place. The complete solid model is used to verify the results output from the spreadsheet. Component and total weights can be compared with those found internally by the spreadsheet. Assembly CG and MOI's can be checked for consistency between the CATIA model and spreadsheet

approximations. Fuel capacity estimates can also be checked with minimal manipulation of the model. This solid model may also be used as the basis for further detailing on the wing and its sub-structure (joints and cutouts) and subsystems.

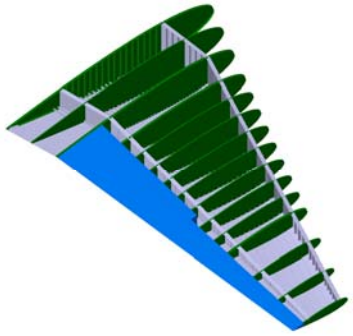

Figure 17. CATIA Optimized Solid Model

C. Automated Abaqus Model

An automated plug-in for the ABAQUS FEA program was scripted in Python. Once activated inside of ABAQUS, the script reads in the optimized planform with a unique model tree designed specifically for the wing problem. The scripting automatically generates a surface model of the optimized wing complete with ribs, spars, skins and all stiffeners (Fig. 18). In addition to geometry the plug-in automatically applies material and section assignments to each surface. Naming convention is standardized for easy recognition where specific assignments can be easily altered by the user. Model navigation is aided by automating surface set assignments. Global sets such as rib surfaces, all spar surfaces, upper skins, and lower skins are created. Local sets down to component webs, caps and stiffeners are also generated.

Figure 18. ABAQUS Model With Section Properties

A second component of the script automatically seeds the model for meshing. This algorithm checks the surface geometry to ensure an adequate number of elements are created regardless of feature size. For example, blade stiffeners are verified to have more than three elements along their height. After the model is seeded, the ABAQUS auto mesher is used to create the mesh. To complete the FEA model set-up, boundary conditions and loads must be applied manually in the ABAQUS GUI.

D. Performance

The overall time-critical performance for the different aspects of the design tool is widely dependent upon the complexity and size of the wing. For example, a greater span wing will likely require more ribs and thus take longer to converge on a solution and longer to generate geometry in CATIA and ABAQUS. But this design tool will allow the user to generate an optimized wing primary structure for a given complex planform including a surface CATIA model, solid CATIA model, and a meshed FEA model that is ready for loads to be applied in less than 155 minutes. Table 3 shows a range of times it takes to complete each operation within the design tool:

Table 3. Completion Times

Description	Time Requirement		Comment
	Min	Max	
Optimization of wing structure	15 sec	120 sec	assumes planform parameters have already been input
Generation of un-optimized surface CATIA model	10 sec	30 sec	
Generation of optimized surface CATIA model	15 sec	45 sec	
Generation of optimized solid CATIA model	5 min	40 min	
Generation of FEA geometry with assigned section properties	15 min	45 min	only works on 32 bit machines
Generation of mesh geometry within FEA model	30 min	60 min	scripting function seeds the model and prepares it for meshing, may require some manual altering when completed

IV. Verification

To verify the design tool output, a test case was developed for optimization and FEA analysis. The test case was developed around a trapezoidal transport planform with a 25 ft semi-span. Two sets of control surfaces were created, one of 25% chord (inboard flaps) and one of 20% chord (outboard ailerons). Two spars were included, with a kink located at the side of body. Forward spar placement is 25% chord at the root and 15% chord at the kink and tip. Aft spar placement is 74% chord at the root and 70% chord at the kink and tip. Landing gear was located forward of the aft spar at the side of body. An additional fixed rib was placed outboard of the landing gear as a fuel termination rib. Four design load cases were used to optimize the wing structure along with an assumed GTOW of 25,000 lbs. A summary of design loads can be found in Table 4.

Table 4. Verification Test Design Load Cases

	Case 1	Case 2	Case 3	Case 4
	Pull-up @ GTOW	Push-over @GTOW	Rolling at GTOW	Landing at GTOW less 40% fuel
Nx (g)	+1.25	+1.25	+0.25	+4.0
Ny (g)	+0.25	+0.25	+0.25	+2.0
Nz (g)	+3.0	-2.0	+1.0	+4.0
Roll Rate (rad/s)	0.0	0.0	3.0	0

2024 Aluminum was used in the spars, ribs, and lower skins while 7475 Aluminum was selected for the upper and LE skins. Material properties for each were identified from Mil-HNDBK 5. The resultant optimized structure contained 15 ribs (Fig. 17) and an overall empty weight of 1008 lbs. Total fuel capacity was estimated at 7979 lbs.

A. FEA Model Creation

After running the ABAQUS model plug-in, all of the wing geometry, section assignments, and mesh seeds were created (Fig. 19). Approximate run time to complete these steps was 25 minutes.

In the design tool the aero load was simplified to be a line load acting at the ¼ chord. For increased accuracy in the FEA model the line load was replaced by a distributed pressure (Fig. 20). First an assumed pressure distribution as a function of chord was characterized and normalized for a total area of one.

Curve fits were then applied to characterize the chord and leading edge fuselage station with respect to BL.

Figure 19. Verification Test ABAQUS Model

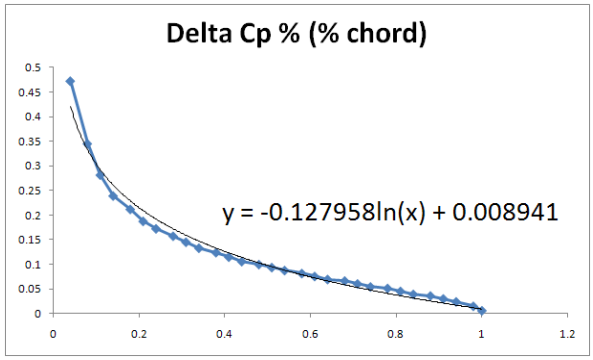

Figure 20. Simplified Distributed Pressure

$$Chord\,(BL) = -.468 \times BL + 190.976 \tag{25}$$

$$LEFS\,(BL) = .577 \times BL + 199.998 \tag{26}$$

Combining these equations the %chord as a function of FS and BL can be determined.

$$\%Chord\,(FS, BL) = \frac{FS - LEFS\,(BL)}{Chord\,(BL)} \tag{27}$$

$$Cp(\%Chord\,) = -.128 \times \ln(\%\,chord\,(FS, BL)) + .0089 \tag{28}$$

Substituting the expression for % chord into the Cp distribution and multiplying by the magnitude of the line load yields an expression for the pressure distribution across the wing. This equation was then input into ABAQUS as an analytical field applied to the upper surface of the wing.

$$P(FS, BL) = \frac{lineload\,(BL)}{Chord\,(BL)} \times Cp(FS, BL) \tag{29}$$

Fuel loads were modeled in ABAQUS using two steps. First, maximum hydrostatic fuel pressures for each rib bay under the desired load case were pulled from the spreadsheet and applied to the surfaces of the fuel tanks. Second, a special inertia was added to the nodes of each fuel tank representing the weight of fuel. The landing gear load was applied as a distributed load along each landing gear rib. The magnitude of the total gear load was taken from the loads spreadsheet of the WDT and converted to a line load for distribution along these two ribs.

Upon completion of the model set up, a mesh was generated using the ABAQUS auto-mesher. Approximate run time to complete the mesh was 42 minutes. The final FEA model had a total of 552,000 shell elements and approximately 3.3 million degrees of freedom.

B. FEA Results

A total of five FEA analyses were completed, one for each design load case and a fifth at 1-g cruise to verify the tip deflection calculations of the design tool. Results for the push-over and rolling maneuver show that neither of these load cases were design critical. Results from the pull-up maneuver show that the stress in each component is almost wholly within material limits (Fig. 21-23). As a preliminary calculation the results prove that globally the design is feasible under the input load conditions. Local hot spots were identified where the ribs and skins come together. Further detailed design will be required to flesh out the structure required at these joints.

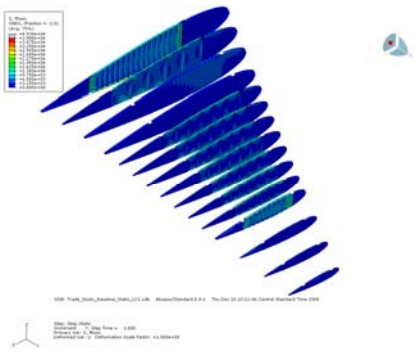

Figure 21. Pull-Up, Ribs Stress Plot

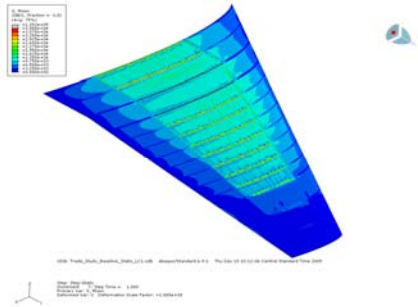

Figure 22. Pull-Up, Lower Skin Stress Plot

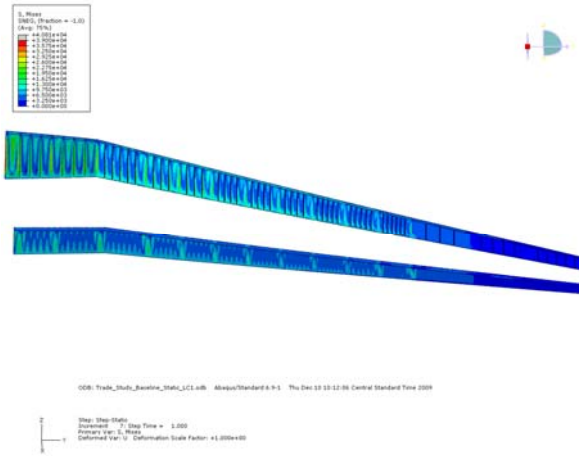

Figure 23. Pull-Up, Spar Stress Plot

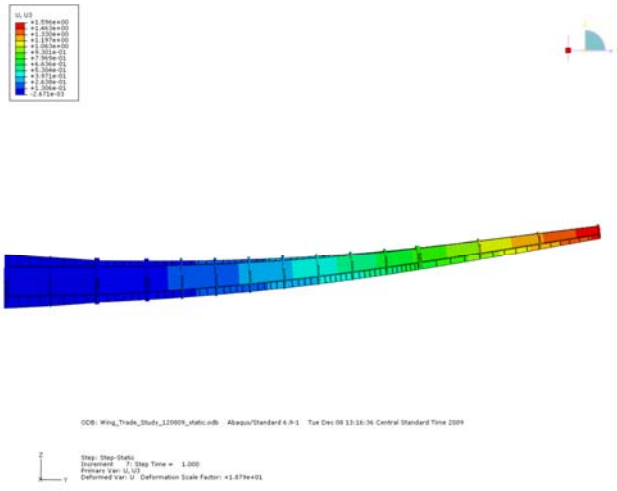

Figure 24. 1-g, Deflection in Z

Results from the 1-g cruise analysis show that the stress in all components is well below the material allowable as expected. Maximum tip deflection calculated by the FEA model for one-g cruise was 1.6 in (Fig. 24). The value calculated by the design tool was 1.5 in, a difference of just -6.25%. This lends a high level of confidence to the tip deflection calculated by the WDT.

V. Future Work

A. Verification Against Legacy Aircraft

Further verification of the design tool is being evaluated for future work. Validation against the FEA model is a step toward validation of the structure based on specified design load cases. The next step is to correlate the design tool weight estimates to as-built airframes. This process will involve researching all the required design tool inputs for multiple legacy aircraft and examining how the results compare with the final production aircraft. Identification of discrepancies between the design tool and as-built aircraft will help refine the calculation methodologies of the optimization procedure.

Final detailed designs will always differ from the idealized shell model of the design tool. To account for this a calibration factor for wing structure weight and available fuel volume has been built into the design tool. Through collection of data comparing the design tool results versus as-built aircraft, potential trends may be identified. A review of these trends could establish values for the design tool calibration factors and establish a higher level of confidence in the final weight and fuel volume predictions.

B. Improving Computational Time

Improved solution techniques can be applied to the structural calculations. The current technique relies on the manufacturing constraints to bound the dimensions of component geometry. Additional pointers and rules of thumb have been incorporated, but much of the design space is searched by brute force looking at all possible combinations. A possible alternative algorithm would actively search the design space by testing the sensitivity of weight and margin to changes in specific component dimensions. Using such a technique, component thicknesses between the current step size limits could be found.

Another computational improvement could be made in the upper limits of the manufacturing constraints. Analysis of as built aircraft could be used to create a regression of typical material thickness versus span, GTOW, or type of aircraft. Limiting the upper bounds would allow the user to search with a finer step size to yield more accurate results. Lower limits would typically be driven by minimum gage production capabilities and remain a required input.

C. Future Enhancements

Potential add-ons to the current design tool could expand the scope of aircraft to be analyzed. Expanding the use of composite materials beyond quasi-isotropic lay-ups would enable more efficient structures in high load designs. Support for honeycomb sandwich panels and specification of fiber angles in laminates are potential additions. Alternate stiffener geometries may also be explored. Current support only allows blade style stiffeners. U, hat, and z style stiffeners are all geometries that could be supported in the future.

D. Expansion of Scope

With the proven effectiveness of the WDT, it would make sense to expand the functionality to include a fuselage and empennage into the design space. This would further refine the weight estimation techniques and further decrease the amount of time it takes to select a conceptual aircraft design and take it to the PDR level.

VI. Conclusion

Current development of the design tool has established a credible alternative methodology to the regression analysis used in conceptual design of aircraft wings. A wide variety of topologies are supported with the ability to alter planform, airfoil, control surfaces, landing gear geometry, spar placements, payloads, and fuel tanks. The calculations for resultant structural weight, CG, MOI, and fuel volume have been verified against a full solid CAD model. Structural feasibility under the design load cases has been established with an FEA verification model.

Future manuscripts will describe how this method, when applied in a multi-disciplinary systems analysis context, can provide design guidance that would seem counter-intuitive if tackled using only a simplified equation set for aerodynamics, weight and performance.

References

[1]Niu, Michael C.Y., Airframe:Stres Analysis and Sizing, 1st ed., Hong Kong Conmilit Press Limited, 1997
[2]Bruhn, E.F., *Analysis and Design of Flight Vehicle Structures, Tri-State Offset Company, 1973*
[3]Beer, Ferdinand P. and Johnston, E. Russell Jr., *Vector Mechanics for* Engineers, 5th ed., McGraw Hill, 1988
[4]Yound, Warren C., *Roarks Formulas for Stress & Strain,* 6th ed., McGraw Hill, 1989